Stability Analysis of an Unbalanced Journal Bearing with Nonlinear Hydrodynamic Forces

Radhouane Sghir and Mnaouar Chouchane

Abstract The research reported in this paper is based on a nonlinear two degree of freedom model of an unbalanced rigid rotor bearing system. The nonlinearity is introduced into the model through closed form expressions of the short bearing hydrodynamic forces. The model in its nondimensional form depends on three nondimensional parameters: the bearing modulus, the rotor rotating speed and unbalance. For the balanced system, numerical continuation is applied to predict the branch of equilibrium positions of the journal and its bifurcation into stable or unstable limit cycles at the linear stability threshold speed. For the unbalanced system, however, numerical integration is used to find the bifurcation diagrams using the rotor speed as a bifurcation parameter. Poincaré sections are used to characterize the journal motion. The investigation is carried out for three bearing parameters covering a large domain of rotor bearing conditions. The effect of unbalance on the journal motion is investigated in each case. Compared to the balanced system, it has been found that unbalance may introduce, at different speed ranges, periodic oscillations at multiple periods of rotation, quasi-periodic oscillations and chaotic motion. The effect of unbalance on journal motion is highlighted and closely related to the bifurcation diagram of the balanced rotor.

Keywords Stability analysis · Numerical continuation · Unbalanced rotor · Nonlinear dynamics · Hydrodynamic bearings

R. Sghir (✉) · M. Chouchane
Laboratory of Mechanical Engineering, National Engineering School of Monastir, University of Monastir, Avenue Ibn Eljazzar, 5019, Monastir, Tunisia
e-mail: sghirradhoineim@yahoo.fr

M. Chouchane
e-mail: mnaouar.chouchane@enim.rnu.tn

P. Pennacchi (ed.), *Proceedings of the 9th IFToMM International Conference on Rotor Dynamics*, Mechanisms and Machine Science 21,
DOI 10.1007/978-3-319-06590-8_88

1 Introduction

Journal bearings are widely used to support the rotors of different types of rotating machines because of their high load and high speed capabilities, high damping and relatively low cost. However, at high rotor speeds, a journal bearing may undergo large instable oscillations due to self excited vibrations which may lead to bearing failure. It is thus essential to predict the onset of instability for a safe operation of journal bearings.

Following the pioneer research of Newkirk and Taylor [1], researchers derived linear models to predict the threshold of stability and constructed the so-called stability charts [2, 3]. Subsequent numerical and experimental researches showed the importance of nonlinear modeling to provide more information about the motion of the rotor in the vicinity of stability threshold [4–7]. Consequently, nonlinear models have been derived for rigid and flexible rotors supported by journal bearings using a variety of models for hydrodynamic forces. Numerical integration is used to predict the motion of the rotor for selected initial conditions. Later, numerical continuation was introduced and used to find the steady state motion of balanced rotors and their bifurcations [7–10]. Unbalance is inherently present in any rotor and should be considered in the modeling. Adiletta investigated numerically and experimentally the effect of unbalance on rotor motion and examined the conditions for which chaotic motion may exist [11–13]. The investigations were generally limited to specific bearing and rotor conditions.

In this paper, we consider a dynamic model of a rigid rotor bearing system. The model depends on three basic nondimensional parameters related to bearing characteristics and loads, unbalance, and rotor speed. The present investigation uses numerical continuation for the balanced rotor as a starting point. The effect of unbalance is then examined for three selected bearing parameters in order cover a large domain of operational conditions. In each case, the effect of unbalance on journal motion and its bifurcation is considered using the rotor rotational speed as a control variable.

2 A Nonlinear Model of an Unbalanced Rigid-Rotor-Bearing System

Consider a rigid rotor supported symmetrically by two identical journal bearings with rigid supports. The bearings are assumed to be aligned and to comply with the short bearing theory. It is also assumed that every point of the rotor undergoes the same lateral motion in a plane perpendicular to the rotor axis of revolution. A section of one bearing is given in Fig. 1a. The position of the journal center O_j with respect to the bearing center O_b is defined in polar coordinates by the eccentricity $e = c\varepsilon$ and the attitude angle ϕ, where ε is the eccentricity ratio and c is the bearing clearance. At constant rotating speed ω, the forces applied on the journal at each

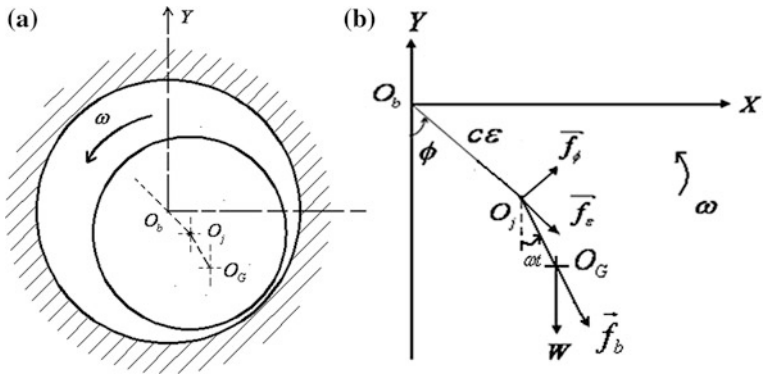

Fig. 1 The journal bearing model: **a** A bearing section. **b** The system of coordinates and forces applied on the journal

bearing, Fig. 1b, are the hydrodynamics fluid film force components $\vec{f}_\varepsilon$ and $\vec{f}_\phi$, respectively in the radial and tangential directions, the weight of the half of the rotor $\vec{W} = M\vec{g}$ and the unbalance force $\vec{f}_b$ with modulus $\left|\vec{f}_b\right| = Ma\omega^2$.

The journal motion is described by two degrees of freedom (ε, ϕ). Applying Newton's second law of motion to the journal, the following two equations of motion are obtained:

$$\begin{cases} \varepsilon'' - \varepsilon\phi'^2 = \dfrac{\omega^2 a}{c}\cos(\omega t - \phi) + \dfrac{g}{c}\cos\phi + \dfrac{f_\varepsilon}{Mc} \\ \varepsilon\phi'' + 2\varepsilon'\phi' = \dfrac{\omega^2 a}{c}\sin(\omega t - \phi) - \dfrac{g}{c}\sin\phi + \dfrac{f_\phi}{Mc} \end{cases} \tag{1}$$

The prime $(')$ in the above equations denotes a derivative with respect to time t.

An explicit relationship between the components of the fluid film force f_ε and f_ϕ and the position and velocity of the journal is used in this paper. The fluid film components are determined by integrating the film pressure distribution derived from the solutions of Reynolds equation using the short bearing theory and the pi-film Sommerfeld boundary condition [14].

$$f_\varepsilon = -\frac{\mu R L^3}{2c^2}\left[\frac{2(\omega - 2\phi')\varepsilon^2}{(1-\varepsilon^2)^2} + \frac{\pi\varepsilon'(1+2\varepsilon^2)}{(1-\varepsilon^2)^{2.5}}\right]$$

$$f_\phi = \frac{\mu R L^3}{2c^2}\left[\frac{\pi(\omega - 2\phi')\varepsilon}{2(1-\varepsilon^2)^{1.5}} + \frac{4\varepsilon'\varepsilon}{(1-\varepsilon^2)^2}\right]$$

The equation of motion (1) may be written in the following nondimensional form:

$$\begin{cases} \ddot{\varepsilon} = \varepsilon\dot{\phi}^2 + \bar{a}\cos(\tau - \phi) + \dfrac{1}{\bar{\omega}^2}\cos\phi + \overline{f_\varepsilon} \\ \ddot{\phi} = -\dfrac{2\dot{\varepsilon}\dot{\phi}}{\varepsilon} + \dfrac{\bar{a}}{\varepsilon}\sin(\tau - \phi) - \dfrac{\sin\phi}{\bar{\omega}^2\varepsilon} + \dfrac{\overline{f_\phi}}{\varepsilon} \end{cases} \tag{2}$$

where, $\dot{(\,)} = d/d\tau = d/\omega dt$ denotes a derivative with respect to nondimensional time $\tau = \omega t$, $\bar{a} = a/c$, $\bar{\omega} = \omega\sqrt{g/c}$ and the nondimensional fluid film force components are defined as: $\overline{f_\varepsilon} = f_\varepsilon/Mc\omega^2$ and $\overline{f_\phi} = f_\phi/Mc\omega^2$.

Using the state variables $x_1 = \varepsilon$, $x_2 = \phi$, $x_3 = \dot{\varepsilon}$, $x_4 = \dot{\phi}$, the system of Eq. (2) may be converted into the following four first order differential equations

$$\begin{cases} \dot{x}_1 = x_3 \\ \dot{x}_2 = x_4 \\ \dot{x}_3 = x_1\dot{x}_2^2 + \bar{a}\cos(\tau - x_2) + \dfrac{\cos x_2}{\bar{\omega}^2} - \dfrac{\Gamma}{\bar{\omega}}\left[\pi x_3\,\dfrac{\left(1 + 2x_1^2\right)}{\left(1 - x_1^2\right)^{5/2}} + 2x_1^2\dfrac{(1 - 2x_4)}{(1 - x_1^2)^2}\right] \\ \dot{x}_4 = -\dfrac{2\dot{x}_1\dot{x}_2}{x_1} + \dfrac{\bar{a}}{x_1}\sin(\tau - x_2) - \dfrac{\sin x_2}{\bar{\omega}^2 x_1} + \dfrac{\Gamma}{x_1\bar{\omega}}\left[\dfrac{\pi(1 - 2x_4)x_1}{2\left(1 - x_1^2\right)^{1.5}} + \dfrac{4x_3x_1}{\left(1 - x_1^2\right)^2}\right] \end{cases} \tag{3}$$

The above nonlinear system of equations depends on three nondimensional parameters: the bearing parameter $\Gamma = \mu RL^3/2Mc^{2.5}g^{0.5}$, the dimensionless rotor speed $\bar{\omega}$ and the nondimensional rotor eccentricity $\bar{a}$, where μ is the lubricant viscosity, R is the journal radius and L is the bearing length.

3 Results

In the following investigations, the bearing parameter Γ and unbalance $\bar{a}$ are first selected and the journal speed $\bar{\omega}$ is used as a control or varying parameter. For a defined values of the three nondimensional parameters in Eq. (3), the motion of the journal center, defined by the polar coordinates ε, ϕ can be determined by numerical integration for a selected initial position of the journal.

To consider the largest range of bearing parameter, three selected values of Γ are considered: 0.02, 0.2, and 2 corresponding respectively to low, moderate and large bearing parameters. For the unbalance, the investigation uses the balanced rotor, $\bar{a} = 0$, as a reference. In this case, the bifurcation diagram is determined using numerical continuation as explained in details in reference [10]. The nondimensional

unbalance is then increased progressively by a step of 0.05 form $\bar{a} = 0$ to $\bar{a} = 0.2$. Five values of the nondimensional unbalance are thus considered (0, 0.05, 0.1, 0.15, 0.2). The objective of the investigation is to determine the effect of unbalance on the motion of the journal at different rotor speeds.

Figure 2 shows the bifurcation diagram of the balanced rotor, $\bar{a} = 0$, for three bearing parameters $\Gamma = 0.02, 0.2$ and 2. At low journal rotational speeds, $\bar{\omega} < \bar{\omega}_H$, the journal center has a stable equilibrium point for which the branch is given in solid line. The equilibrium point undergoes a Hopf bifurcation, noted by the letter "H" in the figure, at the journal speed $\bar{\omega}_H$. The Hopf bifurcation is supercritical for $\Gamma = 0.02$ and 0.2 and subcritical for $\Gamma = 2$. For the supercritical Hopf bifurcation, stable periodic oscillations bifurcate from the Hopf point and undergo a progressive increase of amplitude until the Limit Point of Cycle (LPC) bifurcation is encountered. For the subcritical Hopf bifurcation, unstable limit cycles exist between the Hopf point and the LPC point.

Figure 2 also shows the branches of unstable equilibrium point as dashed lines. The stability threshold is the curve joining the Hopf bifurcation points shown as solid line for the supercritical Hopf bifurcation and as a dashed line for the subcritical Hopf bifurcation. The system is stable for $\bar{\omega} < \bar{\omega}_H$ and unstable for $\bar{\omega} > \bar{\omega}_H$.

Following Hopf supercritical bifurcation, the system undergoes two successive LPC bifurcations for $\Gamma = 0.02$ and $\Gamma = 0.2$ as shown respectively in Figs. 3 and 4. The speed range $\bar{\omega}_{LPC1} - \bar{\omega}_{LPC2}$ is significantly larger for $\Gamma = 0.02$. For $\Gamma = 2$, a single LPC bifurcation is found as shown in Fig. 2.

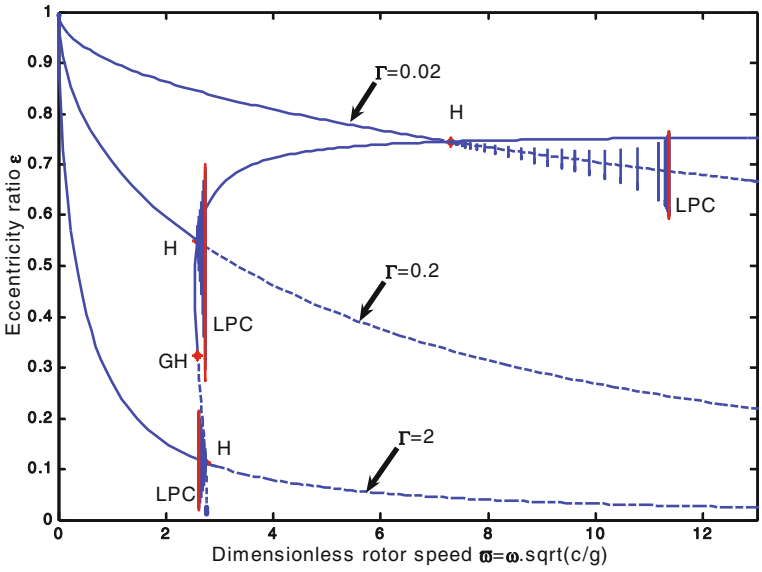

Fig. 2 Bifurcation diagrams for the balanced rotor for three selected bearing parameters $\Gamma = 0.02$, 0.2 and 2

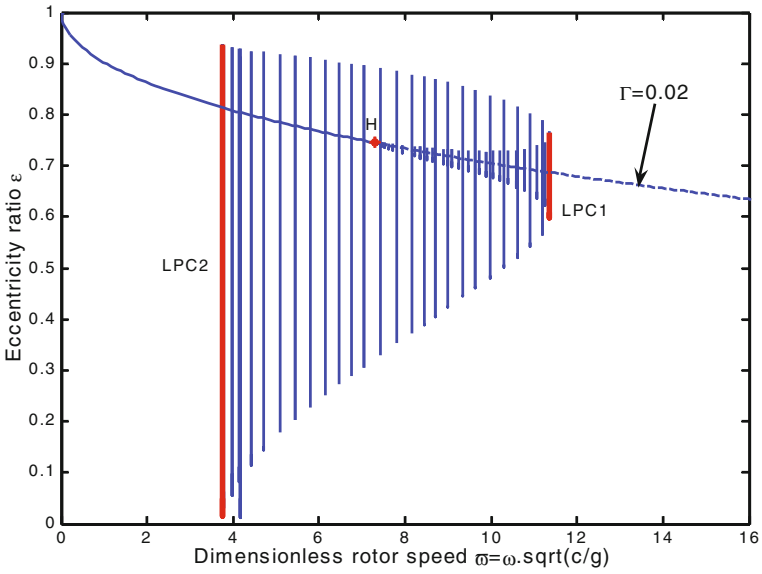

Fig. 3 Bifurcation diagram for $\Gamma = 0.02$

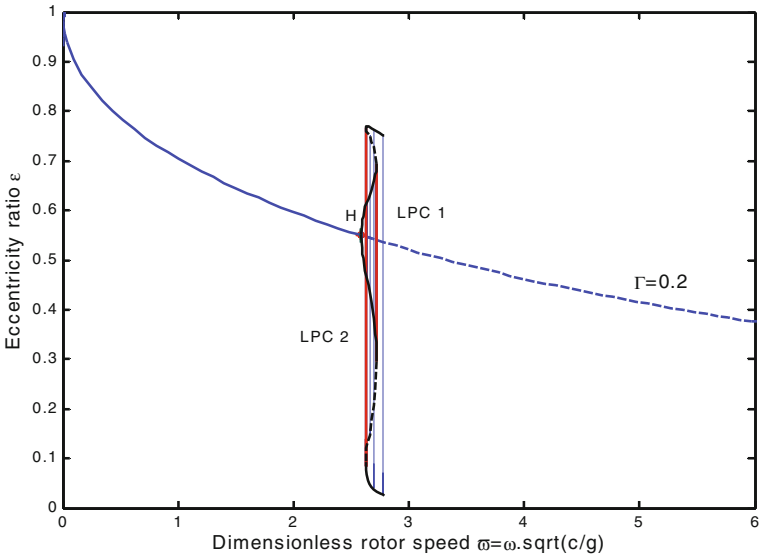

Fig. 4 Bifurcation diagram for $\Gamma = 0.2$

In the following, the effect of unbalance is investigated. The three bearing parameters are considered starting from the low bearing parameter $\Gamma = 0.02$. For each case, the unbalance is increased progressively by a step of $\Delta\bar{a} = 0.05$. In each

case, the bifurcation diagram is found showing the variation of the eccentricity ratio $\varepsilon(t)$ with the control parameters $\bar{\omega}$. The diagram is shown first as orbits sampled at the rotating speed, $\bar{\omega} = 1$ and then is shown as closely spaced trajectory points. Figure 5 shows the bifurcation diagrams for $\Gamma = 0.02$ and $\bar{a} = 0.05$. These diagrams demonstrate that the motion of the journal is T-periodic for $\bar{\omega} < 6.74$ and becomes quasi-periodic for $6.74 < \bar{\omega} < 10.84$. The quasi-periodicity of the motion is justified by the closed curve of the Poincaré map and the unevenly spaced peaks of the spectrum in Fig. 6. For $\bar{\omega} > 10.84$, the orbits becomes 2T-periodic with large oscillations corresponding to $\varepsilon(t)$ close to one.

The motion in Fig. 5 follows very closely the bifurcation diagram of Fig. 2. The major difference is that the motion becomes quasi periodic at the Hopf point rather than periodic. It is clear that the motion jumps to large oscillations with eventual rubbing between the journal and the bearing bush at $\bar{\omega} < 10.84$. Figure 5 implies that, for a low bearing parameters, safe operation is possible up to relatively high rotor speeds as long as unbalance is kept under tight control.

When the unbalance is increased above $\bar{a} = 0.05$, the small quasi-periodic oscillations at speeds higher than $\bar{\omega}_H$ gradually disappear. The journal jumps to large oscillation motion with eccentricity close to 1 at approximately $\bar{\omega} = 3.7$ as shown in Fig. 7 for an unbalance $\bar{a} = 0.15$. The jumping point corresponds to the LPC2 bifurcation shown in Fig. 3. Figure 7 also shows that the motion becomes 2T-periodic in the speed range $2.07 < \bar{\omega} < 2.44$ and quasi-periodic in the vicinity of $\bar{\omega} = 2.97$.

The case of moderate bearing parameter $\Gamma = 0.2$ is now considered. This case is characterised by significantly small speed range for the supercritical stable oscillations shown in Fig. 2 for the balanced case. When unbalance is introduced in the model, T-periodic oscillations are found for $\bar{\omega} < \bar{\omega}_H$ as shown in Fig. 8. The motion jumps to larger 2T-periodic oscillations for $2.32 < \bar{\omega} < 2.53$. This speed range corresponds to the speed interval between the LPC1 and LPC2 points in Fig. 4. At roughly $\bar{\omega} = 2.53$, the journal jumps to large 2T-periodic oscillations with

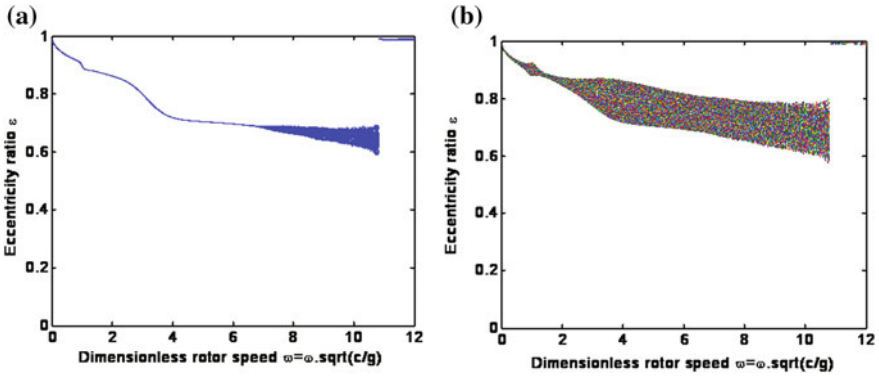

Fig. 5 Bifurcation diagrams for $\Gamma = 0.02$ and $\bar{a} = 0.05$: **a** Journal trajectory sampled at rotor speed. **b** Journal trajectory

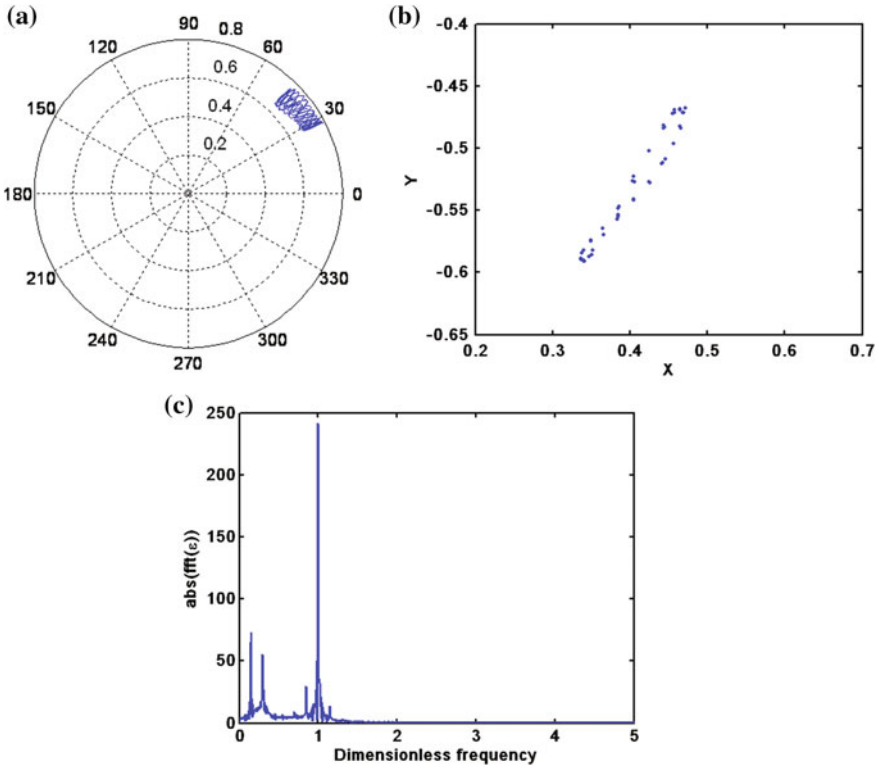

Fig. 6 Journal motion for $\Gamma = 0.02$, $\bar{a} = 0.05$ and $\bar{\omega} = 8.5$: **a** Journal trajectory. **b** Poincarré map and **c** Spectrum

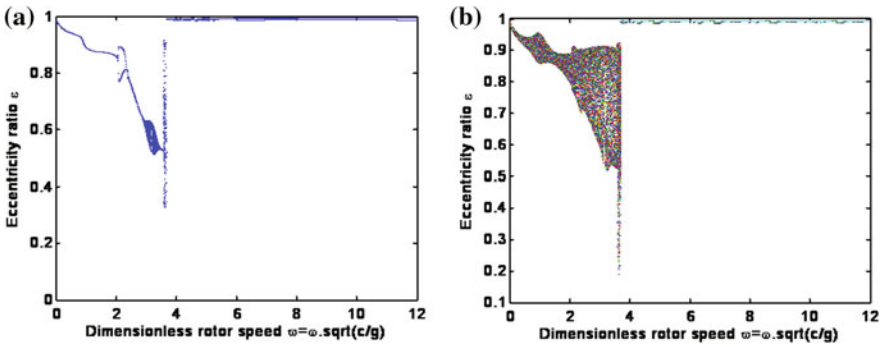

Fig. 7 Bifurcation diagrams for $\Gamma = 0.02$ and $\bar{a} = 0.15$: **a** Journal trajectory sampled at rotor speed. **b** Journal trajectory

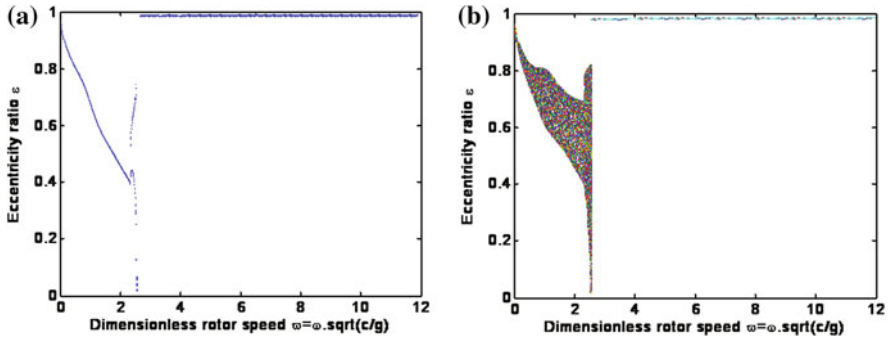

Fig. 8 Bifurcation diagrams for $\Gamma = 0.2$ and $\bar{a} = 0.2$: **a** Journal trajectory sampled at rotor speed. **b** Journal trajectory

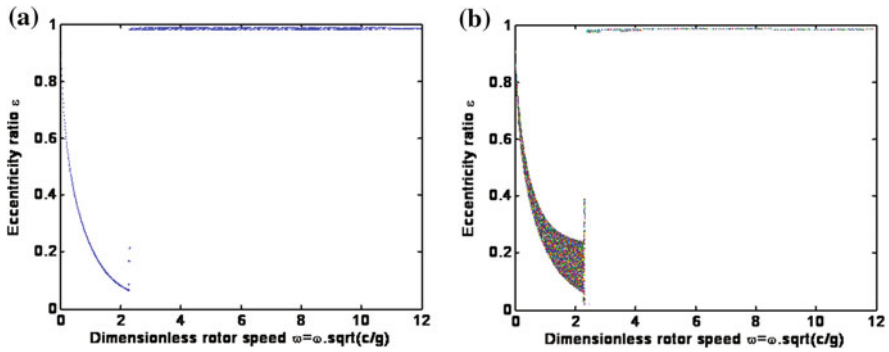

Fig. 9 Bifurcation diagram for $\Gamma = 2$ and $\bar{a} = 0.2$: **a** Journal trajectory sampled at rotor speed. **b** Journal trajectory

eccentricity very close to one. The increase of unbalance in the range $0.05 < \bar{a} < 0.2$ progressively increases the amplitude of the T-periodic oscillations for $\bar{\omega} < \bar{\omega}_H$.

The last considered case corresponds to a bearing parameter $\Gamma = 2$. In this case, an LPC bifurcation occurs at $\bar{\omega} = 2.62$ as shown in Fig. 2 for the balanced case. In the unbalanced case, Fig. 9, the motion becomes T-periodic up to $\bar{\omega} = 2.27$ corresponding to the LPC bifurcation. Then, the oscillations become 2T-periodic with an amplitude increasing rapidly to an eccentricity close to one. The effect of unbalance is essentially to increase the amplitude of the T-periodic oscillations for $\bar{\omega} < \bar{\omega}_H$.

4 Discussion and Conclusion

A two degree of freedom model is used to investigate the effect of unbalance on journal motion at varying rotational speed. The bifurcation diagrams for the balanced rotor, derived by numerical continuation, have been found very valuable to

predict the domain of safe operation. For low bearing parameters, corresponding to low oil viscosity or high static loads, a significant large domain of operational speed is found to be possible for low rotor unbalance. This domain is reduced to less than a half for moderate and high rotor unbalance. The reduction of the speed domain is justified by the presence of two successive limit point of cycle bifurcations for this case. For moderate and high bearing parameters, the stable speed range is almost independent of the level of unbalance though the amplitude of stable oscillations increases with unbalance.

References

1. Newkirk BL, Taylor HD (1925) Shaft whipping due to oil action in journal bearings. G E Rev 28:559–568
2. Holmes R (1960) The vibration of a rigid shaft on short sleeve bearings. J Mech Eng Sci 2:337–341
3. Reddi MM, Trumpler PR (1962) Stability of the high-speed journal bearing under steady load. ASME J Eng Ind 84:351–358
4. Meyers CJ (1986) Bifurcation theory applied to oil whirl in plain cylindrical journal bearings. ASME J Appl Mech 51:244–250
5. Guo JS (1995) Characteristics of the nonlinear hysteresis loop for rotor-bearing instability. Ph. D. thesis, Case Western Reserve University, USA
6. Wang JK, Khonsari MM (2005) On the hysteresis phenomenon associated with instability of rotor-bearing systems. ASME J Tribol 128:188–196
7. Wang JK, Khonsari MM (2006) Bifurcation analysis of a flexible rotor supported by two fluid film journal bearings. ASME J Tribol 128:594–603
8. Boyaci A, Hetzler H, Seeman W, Proppe C, Wauer J (2008) Analytical bifurcation analysis of a rotor supported by floating ring bearings. Nonlinear Dyn 57:497–507
9. Chouchane M, Amamou A (2011) Bifurcation of limit cycles in fluid film bearings. Int J Nonlinear Mech 46:1258–1264
10. Sghir R, Chouchane M (2014) Prediction of the nonlinear hysteresis loop for fluid-film bearings by numerical continuation. J Mech Eng Sci. doi:10.1177/0954406214538618
11. Adiletta G, Guido AR, Rossi C (1996) Chaotic motions of a rigid rotor in short journal bearings. Nonlinear Dyn 10:251–269
12. Adiletta G, Guido AR, Rossi C (1997) Nonlinear dynamics of a rigid unbalanced rotor in journal bearings. Part I: theoretical analysis. Nonlinear Dyn 14:57–87
13. Adiletta G, Guido AR, Rossi C (1997) Nonlinear dynamics of a rigid unbalanced rotor in journal bearings. Part II: experimental analysis. Nonlinear Dyn 14:157–189
14. Frêne J, Nicolas D, Degueurce B, Berthe D, Godet M (1997) Hydrodynamic lubrication bearings and thrust bearings. Elsevier, Tribology Series, Amsterdam